International Journal of Innovative Computing, Information and Control
Volume **15**, Number **5**, October **2019**

 ISSN 1349-4198
pp. 1881–1900

STRUCTURE FROM MOTION RECOVERY FOR MONOCULAR VISION SYSTEMS: A ROBUST NONLINEAR OBSERVER-BASED APPROACH

Zoubaida Mejri[1,3], Lilia Sidhom[1,2] and Afef Abdelkrim[1,3]

[1]Research Laboratory L.A.R.A in Automatic Control
National Engineering School of Tunis (ENIT)
University of Tunis El Manar
BP 37, Le Belvédère, Tunis 1002, Tunisia
zoubaida.mejri@enit.utm.tn; lilia.Sidhom@enib.rnu.tn; afef.a.abdelkrim@ieee.org

[2]National Engineering School of Bizerte (ENIB)
University of Carthage
BP 66, Campus Universitaire Menzel Abderrahman 7035, Bizerte, Tunisia

[3]National Engineering School of Carthage (ENICarthage)
University of Carthage
45 Rue des Entrepreneurs, Charguia II, Tunis 2035, Tunisia

Received February 2019; revised June 2019

Abstract. *This paper deals with the estimation structure and motion of a moving object with time varying velocities viewed by a moving camera problem, in which the object motion is assumed to be on a ground plane. The problem focuses on the dynamics of a relative motion model based on a moving camera and a moving object where disturbances and uncertainties are diagnosed. To treat this problem, the Nonlinear Unknown Input Sliding Mode Observer (NUISMO) is proposed with feedback injection term in addition to giving a proof of its convergence. Lacking information about the nature of model nonlinearities except that is upper bound and its boundary can be generated in real time. The object velocities are considered as an unknown input to the perspective dynamical system. This approach allows decoupling the state object estimation from its velocities that behaves also as a disturbance input. Several simulation results are performed to show the effectiveness of the proposed approach compared to a Nonlinear Unknown Input Observer (NUIO) in the presence of measurement noise.*

Keywords: Structure from motion estimation, Measurement noise, Unknown input observer, Sliding mode, Uncertain nonlinearity, Disturbances

1. **Introduction.** In robotics and computer vision fields, the well-known problem of Structure from motion and Motion from Motion which is referred to as trajectory triangulation [1,2] and is termed to SaMfM [3], is yet addressed today [4-8]. Given one dynamic object that moves throughout a video sequence and given its 2-D tracked features, the aim of the SaMfM is to recover the structure and motion that is represented respectively by the three-dimensional structure of the scene (the Euclidean coordinates) and its motion relative to the camera. SaMfM is often required for numerous applications, for instance, augmented reality, autonomous navigation, video-based surveillance, vision-based robotic applications and object recognition, among others. The interest of solving the SaMfM problem can be explained for example in a practical case by a robotic arm equipped with camera and taking hold of objects moving on a conveyor. Thus, this robot can estimate its own coordinate and motion while sensing its environment which is

DOI: 10.24507/ijicic.15.05.1881

a challenging task. Furthermore, algorithms designed for SaMfM can be used also for face shape reconstruction using a video showing a face changing pose over time. Moreover, for autonomous vehicle in outdoor environment which includes localization estimation, the structure and motion recovery can provide the position of a vehicle, which supports the future navigation.

As can be observed in the literature, many solutions have been developed for the SaMfM problem. These solutions can be classified as two different approaches: an offline and online based approach. In general, the offline methods [9-15] utilize some relationship between 3D coordinates of points in the camera coordinate frame and corresponding 2D projections on image frame. However, they require the collection of at least some numbers of images to estimate the object structure. One of the drawbacks of using an offline approach is that it is not specified as operating in real time. Moreover, the methods based on this approach show a lack of the convergence proof. This explains the need for online structure estimation algorithms.

The online approach relies on the use of a dynamical model. In fact, the methods of such approach can take a data from images in iterative way to each sampling step. Furthermore, these methods do not need some number of point correspondences or views. Various methods are proposed in the literature, such as the multibody structure from motion algorithm [16,17] that allows the recovering of the structure and motion of dynamic scenes with multiple rigidly moving objects. However, this method can yield some issues arise due to different situations, for example, the small moving foreground dynamic objects with few and short feature tracks. A new pipeline dubbed Samantha is designed in [18] that embraces a hierarchical approach. The algorithm is described as a binary tree constructed by agglomerative clustering over the image sequence. It presents better error containment, leading to more stability and uses process frames without ancillary information. The main limitation of these methods is the sensitivity to noise and outliers. Recently, a real-time sequential Bayesian estimation approach is developed based on the extended Kalman filter [19,20] to recover the structure from motion of non-rigid surfaces from a monocular video. Nevertheless, this approach has some defects as it assumes that the state belief is Gaussian distributed. However, with regard to problems encountered, robustness and efficiency are still two most challenging issues. This work is motivated by the realization that existing estimation methods do not often give satisfactory results or even fail in many real-time configurations due to the complexity of implementation or settings. To avoid these problems, an alternative method that exists based on observer designs can be used to address the SaMfM problem. For example, in [21], the authors have proposed to use a reduced order nonlinear observer to estimate the structure of the stationary object seen by a moving calibrated camera. A nonlinear observer is proposed to estimate the structure of moving object from a stream of images captured with a camera having known motion [3]. In this last one, the structure and motion estimations apply some constraints where the linear object velocities observed by a moving camera are supposed as constant. Otherwise, if the object is not moving with constant velocities then the proposed solution cannot be used. To overcome this, an extension work is presented in [22] where a Nonlinear Unknown Input Observer (NUIO) is designed to estimate the structure by considering a moving object with time-varying velocities. The key idea here is that the object's velocities are considered as an unknown input to the perspective dynamical system. However, the theoretical design and simulation results are performed just for a moving camera observing an object moving along a straight line. This proposed method is experimentally performed conducted on a PUMA 560 robot with two degrees of freedom [23]. In return, the method remains limited compared to the object moving. Other works can also be cited, such as in [24] where a Robust Integral Signed Error (RISE)-based robust nonlinear observers

were proposed to estimate the motion of a monocular camera and the range between the moving camera and the object, although the information of these is not admitted in the 2-D camera images. Recently, [25] proposes a complete-order observer for structure and motion estimation assuming only the single component of linear velocity as it is known. To estimate the camera motion, the authors use the well-known Levant's differentiator.

In this paper, a considered scenario is defined by a moving object assumed to be moving along a straight line or in a plane with a priori unknown time varying velocities and observed by a camera with arbitrary motion. This scenario is modelled as a dynamic nonlinear system with unknown inputs and uncertain nonlinearities. First, the unknown inputs such as moving object velocities which can behave as a disturbance input. However, the uncertain nonlinearities are caused by incoherent camera velocity sensor. The essential contribution of our work is to design a robust observer and its existing conditions despite model uncertainties and disturbances. In fact, disturbances and uncertainties are both important issues to be considered in the observer design. The analysis of designing schemes for different classes of nonlinear systems has been studied extensively over the past decades. For example, the authors in [26-28] have developed an extended-state-observer based control strategy to handle the external disturbances and uncertain nonlinearity.

In our research, the proposed method is made from an NUIO adding a sliding mode technique to be robust against specified disturbances and even time-varying uncertainties. Then, the Nonlinear Unknown Input Sliding Mode Observer (NUISMO) is designed with a feedback injection term to upgrade the results. The proposed observer is set by assuming some conditions. Its convergence properties are derived using a Lyapunov function and then LMI based approach is used. A performance comparison study with an NUIO proposed by Dani et al. [22] is undertaken. This letter is chosen as a reference for its robust performance to solve the SaMfM problem.

The main contributions of the present paper can be summarized as follows.

- NUISMO based approach for a monocular vision system with uncertainty is proposed. In comparison to the existing studies, the novelty of the work is in the manner uncertainty is processed.
- The proposed approach assumes a motion of the object as unknown, in the presence of measurement noise and the camera can move in a free way without any limits. However, our approach is in contrast with some previous studies that require prior knowledge of either the motion of the moving object or scene geometry.
- The proposed approach uses upper bound of the nonlinearity which is computed in real time and obtained as byproduct of Lyapunov stability method. Therefore, no information about the nature of the nonlinearity is required.

The rest of this paper is organized as follows. Necessary preliminaries and problem statement are presented in Section 2. In Section 3, a proposed NUISMO is designed and Lyapunov-based analysis is treated to prove asymptotic convergence of estimation error in the presence of model uncertainty. Section 4 shows the simulation results to highlight the interest of the proposed observer. Finally, Section 5 concludes the paper.

2. **State Dynamic Formulation.**

2.1. **Euclidean and image space relationship.**

Let us consider a moving camera shooting feature points of a dynamic object; this letter seems to be moving in the camera reference frame as shown in Figure 1.

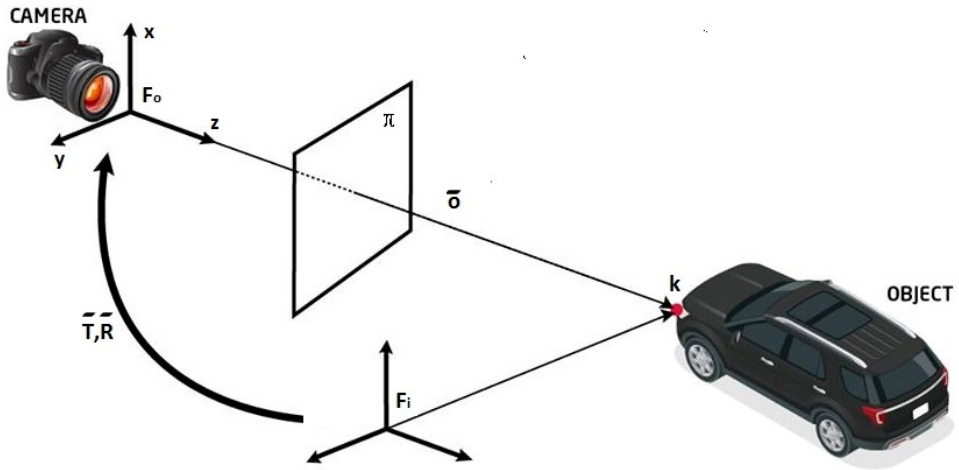

FIGURE 1. Camera-object motion model

Along the measurement model in both Euclidean and image spaces, the point correspondences between successive images of the moving camera need to be defined. These correspondences can be computed using the feature tracking methods [29,30]. After the initial time t_0, F_i an inertial frame identical to F_o attached to the camera moves in a static environment and undergoes some translation $\overline{T}(t) \in \mathbb{R}^3$ and rotation velocity $\overline{R}(t) \in SO(3)$, where $SO(3)$ is the 3D rotation group. First, let us introduce the Euclidean coordinates $\overline{o}(t) \in \mathbb{R}^3$ of a feature point as $\overline{o}(t) = [\ X(t),\ \ Y(t),\ \ Z(t)\ ]^T$ in the camera frame F_o. This coordinate is valid for any point observed by the camera. Then, the normalized Euclidean coordinates are obtained as $o(t) = [\ X(t)/Z(t),\ \ Y(t)/Z(t),\ \ 1\ ]^T$ to reduce the number of unknown components to two. To minimize the complexity of the subsequent development, an auxiliary state vector $x(t) = \left[\ x_1(t),\ \ x_2(t),\ \ x_3(t)\ \right]^T$ is defined instead of $o(t)$ as

$$x = [\ X/Z,\ \ Y/Z,\ \ 1/Z\ ]^T \tag{1}$$

To map a point in the 3D reference frame F_o to the 2D image plane, a projective geometry is used [31]. A relationship between the pixel coordinates in the image space and the normalized Euclidean coordinates $o(t)$ is given by

$$P_x = C_c o \tag{2}$$

with P_x being a vector of the pixel coordinates in the image space given by $P_x = \left[\ u\ \ \ v\ \ \ 1\ \right]^T$ and $C_c \in \mathbb{R}^{3\times3}$ a known invertible camera calibration matrix. Using the relation (2), only the first two components x_1 and x_2 of the state x can be measured, and the third one x_3 is an inverse of the unmeasurable $Z(t)$ (an inverse depth) which is the relative Euclidean distance between the moving camera and the feature point.

2.2. **Structure and motion model.** First, let us present the expression of the feature point k seen by a moving camera in F_o as $\overline{o}(t) = \overline{T} + \overline{R}t_{ok}$ for a vector t_{ok} which starts from the centre of the coordinate frame F_i to k. Its time derivative gives the relative motion [22] between the point k and the camera in F_o as follows

$$\dot{\overline{o}} = [\omega]\overline{o} + v_r \tag{3}$$

where $[\omega] \in \mathbb{R}^{3\times3}$ represents a skew symmetric matrix made from the angular velocities of the camera defined as

$$[\omega] = \begin{bmatrix} 0 & -\omega_3 & \omega_2 \\ \omega_3 & 0 & -\omega_1 \\ -\omega_2 & \omega_1 & 0 \end{bmatrix} \tag{4}$$

and v_r is a relative linear velocity of the camera, expressed by

$$v_r = v_c - v_k \tag{5}$$

with $v_c = \begin{bmatrix} v_{cx} & v_{cy} & v_{cz} \end{bmatrix}^T$ being the camera velocity vector and $v_k = \begin{bmatrix} v_{kx} & v_{ky} & v_{kz} \end{bmatrix}^T$ the point velocity vector expressed respectively in F_o where these velocities are bounded and continuously differentiable. As follows, define $u = \begin{bmatrix} v_c & \omega \end{bmatrix}^T$ a vector which regroups the linear and angular camera velocities. In our case, the vector u and the point velocity vector v_k are assumed to be upper bounded by constants. The subsequent development is based on the design of NUISMO observers for SaMfM to estimate the structure of moving object. This amount estimates the state $x(t)$ of the feature point on the object in each image.

A nonlinear dynamic system can be obtained by substituting ω and v_r into (3) as follows

$$\dot{\bar{o}} = \begin{bmatrix} 1 & 0 & 0 & 0 & Z & -Y \\ 0 & 1 & 0 & -Z & 0 & X \\ 0 & 0 & 1 & Y & -X & 0 \end{bmatrix} \begin{bmatrix} v_r \\ \omega \end{bmatrix} \tag{6}$$

Using the state vector $x(t) = \begin{bmatrix} x_1(t), & x_2(t), & x_3(t) \end{bmatrix}$ and the expression (6), we obtain the dynamics of the $x(t)$ as

$$\begin{aligned} \dot{x}_1 &= -x_1x_2\omega_1 + \omega_2 + x_1^2\omega_2 - x_2\omega_3 + (v_{cx} - x_1v_{cz})x_3 - v_{kx}x_3 + x_1v_{kz}x_3 \\ \dot{x}_2 &= -\omega_1 - x_2^2\omega_1 + x_1x_2\omega_2 + x_1\omega_3 + (v_{cy} - x_2v_{cz})x_3 - v_{ky}x_3 + x_2v_{kz}x_3 \\ \dot{x}_3 &= -v_{cz}x_3^2 - (x_2\omega_1 - x_1\omega_2)x_3 + v_{kz}x_3^2 \\ y &= \begin{bmatrix} x_1 & x_2 \end{bmatrix}^T \end{aligned} \tag{7}$$

The above dynamics take the following general form

$$\begin{aligned} \dot{x} &= F(u, x, y) \\ y &= h(x) \end{aligned} \tag{8}$$

The specific SaMfM dynamics defined by (8) has no clue about the object velocities. To re-write Equation (7) with only measurable states by separating camera velocities u from those of the supposed unknown object, the following systems can be defined

$$\begin{cases} g_1(u,y) \triangleq -x_1x_2\omega_1 + \omega_2 + x_1^2\omega_2 - x_2\omega_3 \\ g_2(u,y) \triangleq -\omega_1 - x_2^2\omega_1 + x_1x_2\omega_2 + x_1\omega_3 \\ g_3(u,y) \triangleq 0 \end{cases}$$
$$\begin{cases} f_1(x,u) \triangleq (v_{cx} - x_1v_{cz})x_3 \\ f_2(x,u) \triangleq (v_{cy} - x_2v_{cz})x_3 \\ f_3(x,u) \triangleq -v_{cz}x_3^2 - (x_2\omega_1 - x_1\omega_2)x_3 \end{cases} \tag{8.1}$$
$$\begin{cases} d_1(x) \triangleq -v_{kx}x_3 + x_1v_{kz}x_3 \\ d_2(x) \triangleq -v_{ky}x_3 + x_2v_{kz}x_3 \\ d_3(x) \triangleq v_{kz}x_3^2 \end{cases}$$

where the sub-functions $g_1(u,y)$, $g_2(u,y)$, $g_3(u,y)$, $f_1(x,u)$, $f_2(x,u)$, $f_3(x,u)$, $d_1(x)$, $d_2(x)$, $d_3(x) \in \mathbb{R}$.

Therefore, the dynamic Equation (8) can be given in the nonlinear system form as follows

$$\begin{aligned} \dot{x} &= f(x,u) + g(u,y) + Dd \\ y &= Cx \end{aligned} \tag{9}$$

where $x(t) \in \mathbb{R}^n$ is the state vector, $u(t) \in \mathbb{R}^m$ a known input defined by the camera velocities, $d(t) \in \mathbb{R}^q$ an unknown input defined by the point, $y(t) \in \mathbb{R}^p$ the output vector, $g(u,y) \in \mathbb{R}^n$ is a function of the first two known components of x and $f(x,u) : \mathbb{R}^n \to \mathbb{R}$ is the nonlinear function which satisfies the Lipschitz condition. Matrix $D \in \mathbb{R}^{n\times q}$ is the unknown input matrix and $C \in \mathbb{R}^{p\times n}$ is the output matrix.

It is assumed that there exists $h > 0$ for the operating range of the state $x(t)$ and the vector $u(t)$ where $\sup |f(x,u)| < h$. Furthermore, it can be obtained that $\sup |f(x,u) - f(\hat{x},u)| < \beta_1$ where β_1 is a positive unknown constant. To facilitate the development of NUISMO design, the system (9) is transformed into the following form

$$\begin{aligned} \dot{x} &= Ax + \overline{f}(x,u) + g(u,y) + Dd \\ y &= Cx \end{aligned} \tag{10}$$

where $\overline{f}(x,u) = f(x,u) - Ax$ and matrix $A \in \mathbb{R}^{n\times n}$ represents the linear part of the system dynamics. The function $\overline{f}(x,u)$ is defined by $\sup |f(x,u) - f(\hat{x},u) - A(x-\hat{x})| \leq \beta_1 + \beta_2$ where β_1 and β_2 are positive unknown constants. These constants are represented respectively by the inequalities below $\sup |f(x,u) - f(\hat{x},u)| < \beta_1$ and $\sup |A(x-\hat{x})| < \beta_2$. In this paper, to recover the 3D structure of the moving object, it is necessary to estimate $x(t)$. The two bounds on nonlinear function β_1 and β_2 are assumed to be unknown and can be estimated in real time. In the next section, structure and motion are estimated using an NUISMO despite uncertainties and disturbances and in the presence of unknown input.

3. Structure and Motion Estimation.

The study of observability is closely related to observer NUISMO design, the following definition of observability of the dynamic system in (10) is based on the indistinguishable concept mentioned in [32].

Definition 3.1. *We consider the system in the general form (8) with $x(0) = x_0$, for an n-dimensional nonlinear system, the sufficient observability condition $rank(O_b) = n$ is satisfied, where*

$$O_b = \begin{pmatrix} dh \\ dL_F h \\ \vdots \\ dL_F^{n-1} h \end{pmatrix} \tag{11}$$

and $L_F h$ represents the Lie derivative of h along F given by $L_F h = \frac{\partial F(x)}{\partial x} h(x)$.

Thus, there are two cases where SaMfM dynamics defined by (10) are not observable: either when the camera advances along the ray projected by the feature point k on the 2D image; in this case, the following equalities are held $v_{cx} - v_{kx} - x_1 (v_{cz} - v_{kz}) = v_{cy} - v_{ky} - x_2 (v_{cz} - v_{kz}) = 0$ or when the camera is fixed, so all camera velocities are canceled $u = 0$. For the rest of the study, the system (10) is observable and the following conditions are satisfied.

(i) D is assumed to be column rank matrix.
(ii) $rank(CD) = rank(D) = q$.

An NUISMO with feedback injection term v_a is proposed as

$$\begin{aligned} \dot{z} &= Nz + Ly + M\overline{f}(\hat{x},u) + Mg(u,y) + Mv_a \\ \hat{x} &= z - Ey \end{aligned} \tag{12}$$

where $\hat{x}(t) \in \mathbb{R}^n$ is the estimate state vector, $z(t) \in \mathbb{R}^n$ the observer state vector, v_a is the feedback injection term that must be designed, $N \in \mathbb{R}^{n\times n}$, $L \in \mathbb{R}^{n\times p}$, $E \in \mathbb{R}^{n\times p}$ and $M \in \mathbb{R}^{n\times n}$ are the observer's parameters of appropriate dimension [33,34] and are designed as below

$$\begin{aligned} N &= (I + EC)A - KC \\ L &= K(I + CE) - (I + EC)AE \\ M &= I + EC \end{aligned} \tag{13}$$

The design of the matrices K and E are explained subsequently. The observer state estimation error is written as follows

$$e(t) = \hat{x}(t) - x(t) = z - Ey - x = z - Mx \tag{14}$$

and its time derivative as $\dot{e} = \dot{z} - (I + EC)\dot{x} = \dot{z} - M\dot{x}$.

Replacing the dynamics of x and z from (10) and (12), error dynamic yields

$$\dot{e} = Ne + (NM + LC - MA)x + M\left(\overline{f}(\hat{x}, u) - \overline{f}(x, u)\right) - MDd + Mv_a \tag{15}$$

For NUISMO (10), the estimated states $\hat{x}$ must converge to the system state x which means that the error dynamics $\dot{e}(t)$ in (15) must converge to zero. Furthermore, it is required that

$$N < 0 \tag{16}$$

$$NM + LC - MA = 0 \tag{17}$$

Referring to the last equation of (13), E is to be found such that

$$(I + EC)D = MD = 0 \tag{18}$$

Indeed, to satisfy the condition of $ECD = -D$ by having adequate solution for parameter E, the conditions (i) and (ii) which are mentioned in the beginning of the paragraph should be satisfied. If (CD) is full column rank, then all the possible solutions of the matrix E can be given in a generalized inverse form [33].

$$E = F + YG \tag{19}$$

where $Y \in \mathbb{R}^{n\times p}$ is an arbitrary designed matrix, $F = -D(CD)^+$ and $G = (I_p - (CD)(CD)^+)$.

Now, the problem is restructured to find Y and K to satisfy (10) and to design the feedback injection term v_a which is necessary for the stabilization of the error dynamics $\dot{e}(t)$ without the knowledge of the upper bounds β_1 and β_2. Here the LMI based approach is used to derive the structure of the NUISMO.

Theorem 3.1. *If there exist matrices P_1, P_2 and $P > 0$ such that*

$$A^T(I + FC)^T P + P(I + FC)A + A^T C^T G^T P_1^T + P_1 GCA - C^T P_2^T - P_2 C < 0 \tag{20}$$

where $P_1 = PY$ and $P_2 = PK$, then, the error dynamics under the influence of the feedback injection term

$$v_a = -\left(\hat{\beta}_1 + \hat{\beta}_2\right) sign\left(M^T P_v e\right) \tag{21}$$

tend to zero asymptotically for any $e(0)$, where $\hat{\beta}_1$ and $\hat{\beta}_2$ are respectively the estimates of β_1 and β_2 computed adaptively as per the following expressions

$$\dot{\hat{\beta}}_1^T = \left\| e^T P_v M \right\| \tag{22a}$$

$$\dot{\hat{\beta}}_2^T = \left\| e^T P_v M \right\| \tag{22b}$$

where P_v is a symmetric positive definite matrix.

Proof: As mentioned above, using the definitions in (16)-(18) the error dynamics in (13) takes the form

$$\dot{e} = Ne + M\left(\overline{f}\left(\hat{x}, u\right) - \overline{f}\left(x, u\right)\right) + Mv_a \tag{23}$$

As it is well known that if $N < 0$, then there exists matrix $P > 0$ to satisfy this inequality [35]:

$$N^T P + PN < 0 \tag{24}$$

Now, replacing the expression of N (11) in (24), one can obtain

$$\left(A^T(I + EC)^T - C^T K^T\right) P + P((I + EC)A - KC) < 0 \tag{25}$$

After bringing the value of E from (19) in (25), this allows to find inequality (20)

$$A^T(I + FC)^T P + P(I + FC)A + A^T C^T G^T P_1^T + P_1 GCA - C^T P_2^T - P_2 C < 0$$

where $P_1 = PY$ and $P_2 = PK$.

Using Schur's complement [36], the above inequality can be converted into the matrix inequality

$$\begin{bmatrix} Z^T + Z & 0 \\ 0 & -P \end{bmatrix} < 0 \tag{26}$$

where $Z = P((I + FC)A) + P_1 GCA - P_2 C$.

The LMI feasibility can now be easily solved using standard LMI algorithm and the observer's parameters can be found satisfying the requisite conditions. The next step is to prove that the feedback injection term v_a expressed in (21) can stabilize the error dynamics to finally achieve the origin and that the error trajectories move towards the sliding surface to stay on this one.

Let us define the sliding surface by

$$s = MP_v e \tag{27}$$

Let us take Lyapunov function candidate as follows

$$V = s^T s + \tilde{\beta}_1^T M^T P_v M \tilde{\beta}_1 + \tilde{\beta}_2^T M^T P_v M \tilde{\beta}_2 \tag{28}$$

with $P_v > 0$, $M^T P_v M > 0$ and the estimation errors $\tilde{\beta}_1$ and $\tilde{\beta}_2$ for the unknown boundaries are defined as $\tilde{\beta}_1 = \beta_1 - \hat{\beta}_1$ and $\tilde{\beta}_2 = \beta_2 - \hat{\beta}_2$ respectively.

The expression (28) can be written using (27) as

$$V = e^T P_v M M^T P_v e + \tilde{\beta}_1^T M^T P_v M \tilde{\beta}_1 + \tilde{\beta}_2^T M^T P_v M \tilde{\beta}_2 \tag{29}$$

Taking the time derivative of (29) along the trajectories of (23) yields

$$\begin{aligned} \dot{V} = {} & e^T \left[N^T P_v M M^T P_v + P_v M M^T P_v N\right] e \\ & + 2e^T P_v M M^T P_v M \left(\overline{f}(\hat{x}, u) - \overline{f}(x, u)\right) \\ & + 2e^T P_v M M^T P_v M v_a - 2\dot{\hat{\beta}}_1^T M^T P_v M \tilde{\beta}_1 - 2\dot{\hat{\beta}}_2^T M^T P_v M \tilde{\beta}_2 \end{aligned} \tag{30}$$

Use the straightforward application of a quadratic Lyapunov function to stability results (24) and consider the fact that the matrix $Z = X^T X$ is positive definite where $Z \in S^{m \times m}$, $X \in \mathbb{R}^{n \times m}$, with $S^{m \times m}$ being a domain of symmetric matrices of dimension $m \times m$. The condition in (24) can be written as

$$N^T P_v M M^T P_v + P_v M M^T P_v N = -Q_s \tag{31}$$

where $Q_s > 0$.

Therefore, the expression in (30) is written as

$$\begin{aligned} \dot{V} \leq {} & -e^T Q_s e + 2\left\|e^T P_v M\right\| M^T P_v M \left\|\overline{f}(\hat{x}, u) - \overline{f}(x, u)\right\| \\ & + 2e^T P_v M M^T P_v M v_a - 2\dot{\hat{\beta}}_1^T M^T P_v M \tilde{\beta}_1 - 2\dot{\hat{\beta}}_2^T M^T P_v M \tilde{\beta}_2 \end{aligned} \tag{32}$$

Now, using the above results and the feedback injection term v_a (21) in (32), one can get

$$\begin{aligned}\dot{V} \leq & -\lambda_{\min}(Q_s)\|e\|^2 + 2\left\|e^T P_v M\right\| M^T P_v M\left[\beta_1 + \beta_2\right] \\ & - 2\left\|e^T P_v M\right\| M^T P_v M\left[\hat{\beta}_1 + \hat{\beta}_2\right] \\ & - 2\dot{\hat{\beta}}_1^T M^T P_v M\left[\beta_1 - \hat{\beta}_1\right] - 2\dot{\hat{\beta}}_2^T M^T P_v M\left[\beta_2 - \hat{\beta}_2\right]\end{aligned} \tag{33}$$

Using the adaptation laws (22a) and (22b) in the previous expression, (33) becomes

$$\begin{aligned}\dot{V} \leq & -\lambda_{\min}(Q_s)\|e\|^2 + 2\left\|e^T P_v M\right\| M^T P_v M\left[\beta_1 + \beta_2\right] \\ & - 2\left\|e^T P_v M\right\| M^T P_v M\left[\hat{\beta}_1 + \hat{\beta}_2\right] \\ & - 2\left\|e^T P_v M\right\| M^T P_v M\left[\beta_1 - \hat{\beta}_1\right] - 2\left\|e^T P_v M\right\| M^T P_v M\left[\beta_2 - \hat{\beta}_2\right]\end{aligned} \tag{34}$$

thus,

$$\dot{V} \leq -\lambda_{\min}(Q_s)\|e\|^2 \tag{35}$$

where $\lambda_{\min}(Q_s)$ is the minimum Eigen value of Q_s.

As a conclusion, we can distinguish that V in (28) is a differentiable, positive definite, radically unbounded function and its assumed derivative $\dot{V}$ is a negative semi definite function. So, it may be that Lyapunov function $V(t)$ is upper bounded by $V(0)$. It further entails that all signals e, β_1 and β_2 are ultimately bounded. Using Barbalat's lemma [37] and the fact that the nonlinear function in (10) is bounded, it may be concluded that $e(t)$ converges in close proximity of sliding mode surface s and approach the origin as t tends to ∞. Additionally, the feedback injection term v_a is undoubtedly the effort to preserve the sliding motion. Finally, $\dot{\hat{\beta}}_1$ and $\dot{\hat{\beta}}_2$ are functions of error e and therefore convergent to constant value. To sum up, the procedure for synthesizing NUISMO can be described as an algorithm as follows.

Step 1: find the parameters K, Y and $P > 0$ by solving LMI feasibility (20).
Step 2: use the results of Step 1 to evaluate E from (19).
Step 3: estimate the observer's parameters N, L and M from (13).
Step 4: find $P_v > 0$ by solving the sufficient condition in (31).
Step 5: design the robust feedback injection term v_a by using the value of P_v.

Contrarily to existing nonlinear observers, the robust feedback injection term based on sliding mode technique in Step 5 was configurated by using the estimates of β_1 and β_2 and the observer state estimation error (see Theorem 3.1).

4. **Simulation Results.** In this section, simulations are performed to validate the proposed method of designing NUISMO. The presented approach estimates the structure of a moving object using the images of a single moving camera which can be taken in real time. The camera calibration matrix C_c is given below

$$C_c = \begin{bmatrix} 720 & 0 & 320 \\ 0 & 720 & 240 \\ 0 & 0 & 1 \end{bmatrix}$$

Simulation results are validated in the presence of uncertainties and under the influence of significant noise. Two different parts are considered and NUISMO performance is evaluated for both cases: In the first instance, a comparative study with an NUIO as known in the literature, especially the one used in [22] chosen as a reference for its performance to solve the considered issue. Then, an expanded study is developed to approve the performance of the proposed observer. Unlike existing studies in the literature, it was

elaborated when all velocity measurements are noisy and the object is moving along a plane. For the simulation tests, SIMULINK is used with sampling period $t_s = 10^{-3}$ s.

4.1. **Comparative study.** Consider the camera motion model in [22], where a dynamic object moves in a straight line. Matrices A, C and D of the system (9) are chosen as

$$A = \begin{bmatrix} 0 & -1 & 2 \\ 1 & 0 & 1 \\ 0 & 0 & 0 \end{bmatrix}, \; C = \begin{bmatrix} 1 & 0 & 0 \\ 0 & 1 & 0 \end{bmatrix} \text{ and } D = \begin{bmatrix} 1 \\ 0 \\ 0 \end{bmatrix}$$

Camera and object velocities are given by

$$v_k = \begin{bmatrix} 0.5\cos(2\pi t/6) \\ 0 \\ 0 \end{bmatrix} \text{ (m/s)} \; , \; v_c = \begin{bmatrix} 2 \\ 1 \\ 0.5\cos(t/2) \end{bmatrix} \text{ (m/s)}$$

$$\omega = \begin{bmatrix} 0 & 0 & -\pi/30 \end{bmatrix}^T \text{ (rad/s)}$$

where v_k, v_c, ω are the point velocity, the linear camera velocity and the angular camera velocity respectively. The time-varying velocity v_k was chosen thereby since the object is moving along the x-axis. As the camera moves in a free way, its linear velocity has components on the three axes of the camera frame, unlike the angular velocity which has a single component on the z-axis.

The gain matrices in [22] are calculated using the LMI feasibility in Matlab and are given by

$$K = \begin{bmatrix} 1.0045 & -0.0000 \\ -0.0000 & 1.0045 \\ -1.0047 & -0.0000 \end{bmatrix}; \quad Y = \begin{bmatrix} 0 & -0.0000 \\ 0 & -1.0000 \\ 0 & -1.0047 \end{bmatrix}$$

And in the proposed observer, all matrices are found as stated below

$$E = \begin{bmatrix} -1.0000 & 0.0000 \\ 0 & -0.600 \\ 0 & -0.5000 \end{bmatrix}, \; M = \begin{bmatrix} 0 & 0.0000 & 0 \\ 0 & 0.4000 & 0 \\ 0 & -0.5000 & 1.0000 \end{bmatrix}$$

$$L = \begin{bmatrix} 0.0000 & 0.0800 \\ 0.4000 & 0.4000 \\ -0.5000 & -0.0900 \end{bmatrix} \text{ and } N = \begin{bmatrix} -0.5000 & -0.2000 & 0.0000 \\ 0.2000 & -0.5000 & 0.4000 \\ -0.0000 & -0.4000 & -0.5000 \end{bmatrix}$$

The matrix $P_v > 0$ is found by solving the sufficient condition LMI's in (31).

$$P_v = \begin{bmatrix} 50.5199 & 0.000 & 0.0000 \\ 0.0000 & 50.5199 & 0.0000 \\ 0.0000 & 0.0000 & 50.5199 \end{bmatrix}$$

For a simulation purpose, the initial target feature point position is set to be $x(t_0) = \begin{bmatrix} 5 & 2 & 1 \end{bmatrix}^T$ (m). Since the initial target feature point position is not known to the observer, so the system and observer start from different initial conditions. The initial condition for the observer is taken as $\hat{x}(t_0) = \begin{bmatrix} -1 & -0.5 & -0.2 \end{bmatrix}^T$ (m). This comparative study is mainly based on the estimation of the inverse depth x_3 which is the relative Euclidean distance between the camera and the feature point.

Table 1 summarizes the RMS (Root Mean Square) error values obtained with the proposed observer and the NUIO [22]. Initial trial is considered with noise free case. After that, a band-limited white noise is added to the measured camera linear velocity with zero mean and a noise power equal to 0.01. In fact, the addition of noise on camera linear velocity is obvious since in practice the measuring instrument inevitably introduces

disturbances. Note that the measurement noise values considered in this comparative study are not studied in [22].

TABLE 1. Comparison table of RMS error values obtained with NUIO in [22] and the proposed scheme

Observer	x_3	x_3 with noisy V_c
NUIO	0.0875	0.0894
Proposed	0.0175	0.0178

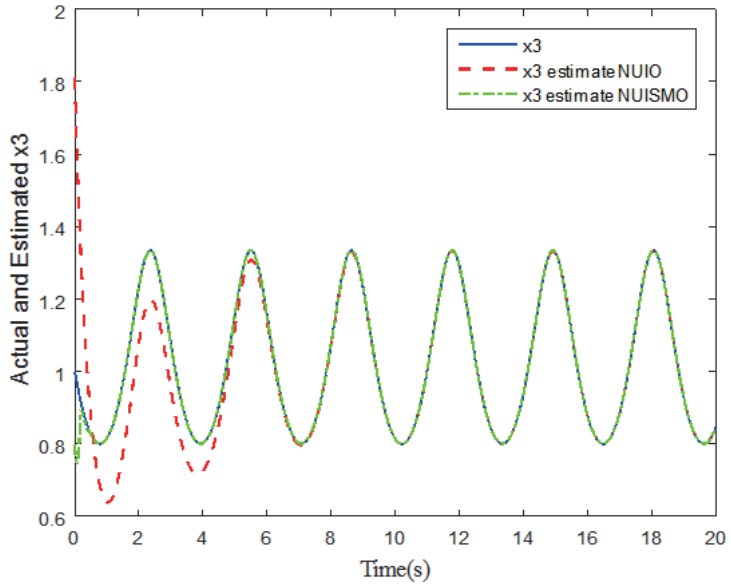

FIGURE 2. Proposed observer state estimate comparison with the NUIO and the real state

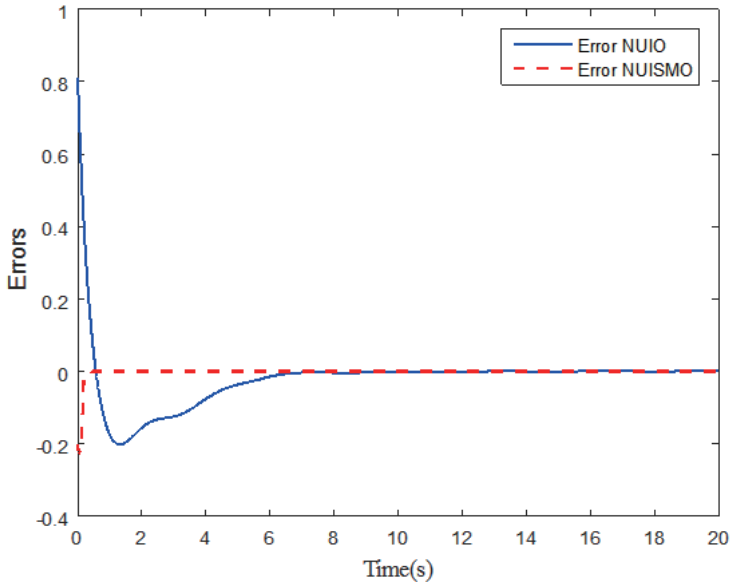

FIGURE 3. Inverse depth estimation error comparison

With regard to the performance comparison study with the NUIO in [22], the steady-state estimation errors are significantly lower with the NUISMO compared to the NUIO. The error values are increased by 5 times compared to that given by the NUIO.

Figures 2 and 3 describe the actual inverse depth, its estimated and the inverse depth estimation error respectively using in both the NUIO and the proposed observer. Figures 4 and 5 show the same results but taking account of the measurement noise on the linear camera velocity. We notice that the transient performance of the NUISMO is significantly

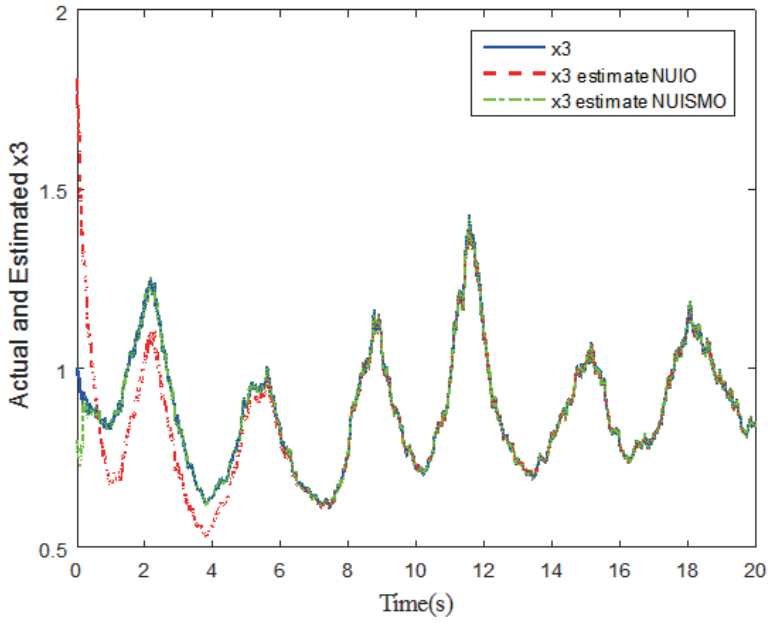

FIGURE 4. Proposed observer state estimate comparison with the NUIO and the real state in the presence of measurement noise

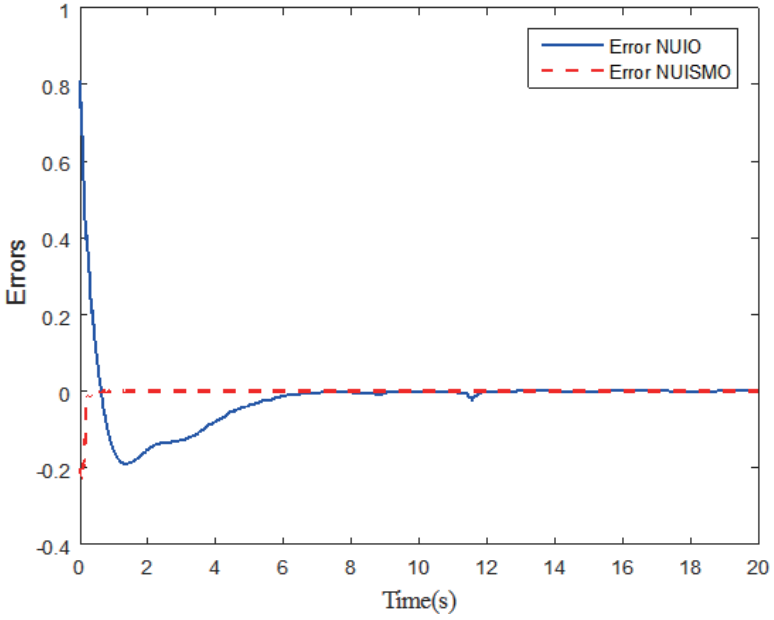

FIGURE 5. Inverse depth estimation error comparison in the presence of measurement noise

superior to the NUIO. So clearly then, the proposed observer has slight superior noise rejection properties and less transient response compared to the observer in [22].

4.2. **Expanded study.** In this part of simulation, the proposed observer is strongly approved by adding a significant measurement noise to both camera and object velocities. Unlike the previous comparative study, the object and the camera can move in a free way without any limits and the object moves on a plane. Three cases are taken, the details of the study are described as follows: First of all, the ideal case (Case 1), also called the noiseless case when the velocity measurements are perfect without any disturbances. Then, the proposed approach is validated for robustness by adding a white noise. Indeed, two cases are given:

- Case 2, uncertainties on the dynamic system are considered precisely in the $f(x,u)$ (see (19)). In fact, these uncertain nonlinearities are caused by the presence of noise on the linear camera velocities (see Figure 9).
- Case 3, we add to Case 2 disturbances that are presented on the unknown input. These disturbances are introduced as noise on the object velocities (see Figure 14).

Matrices A, C and D of the system (9) are given by

$$A = \begin{bmatrix} 0 & -1 & 2 \\ 1 & 0 & 1 \\ 0 & 0 & 0 \end{bmatrix}, \; C = \begin{bmatrix} 1 & 0 & 0 \\ 0 & 1 & 0 \end{bmatrix} \text{ and } D = \begin{bmatrix} 1 & 0 & 0 \\ 0 & 1 & 0 \end{bmatrix}^T$$

The parameters of the object and the camera are chosen in a way to be the closest to the real measurement

$$v_k = \begin{bmatrix} -0.5\cos(\pi t/4) \\ -1 + 0.2\cos(\pi t/8) \\ 0 \end{bmatrix} \text{ (m/s)}, \quad v_c = \begin{bmatrix} \sin(\pi t/4) \\ 1.2 + \sin(\pi t/6) \\ -1 + 0.5\sin(\pi t/8) \end{bmatrix} \text{ (m/s)}$$

$$\text{and } \omega = \begin{bmatrix} 0 & 0 & -\pi/30 \end{bmatrix}^T \text{ (rad/s)}$$

In the proposed observer, all matrices are found as stated below

$$E = \begin{bmatrix} -1 & 0 & 0 \\ 0 & -1 & 0 \\ 0 & 0 & 0 \end{bmatrix}, \quad M = \begin{bmatrix} 0 & 0 & 0 \\ 0 & 0 & 0 \\ 0 & 0 & 1 \end{bmatrix}, \quad L = \begin{bmatrix} 0 & 0 & 0 \\ 0 & 0 & 0 \\ 0 & 0 & 0.5 \end{bmatrix}$$

$$\text{and } N = \begin{bmatrix} -0.5 & 0 & 0 \\ 0 & -0.5 & 0 \\ 0 & 0 & -0.5 \end{bmatrix}$$

The feedback injection term v_a and estimated upper bounds are evaluated as (21). The matrix $P_v > 0$ is found by solving the sufficient condition LMI's in (31).

$$P_v = \begin{bmatrix} 2.3194 & 0 & 0 \\ 0 & 2.3194 & 0 \\ 0 & 0 & 2.6528 \end{bmatrix}$$

Despite the unknown upper bounds of uncertainties and disturbances, the proposed observer NUISMO (12) is used to estimate the position of the object and generate the upper bound of the nonlinearity in real time. Figure 6 shows the curves of the estimate of bounds on nonlinear function in (10). The upper bounds β_1 and β_2 converge to constant value 0.652 after 4 s. An adjustment of the P_v and M offers improvements in convergence.

Case 1: ideal case

Let us start with the first case where it is supposed to have reliable sensors for velocities measurements without disturbances and uncertainties. Figure 7 describes the actual and estimated moving object position. Figure 8 presents the curves of structure estimation errors where these last ones are the difference between the estimated and the actual states. Note that the error values obtained in this case are quite small and they are presented as follows: $er_1 = -9.09 \times 10^{-6}$, $er_2 = -2.27 \times 10^{-5}$ and $er_3 = 0.1 \times 10^{-7}$, where er_1, er_2, er_3 are errors of 1^{st}-state, 2^{nd}-state and 3^{rd}-state respectively.

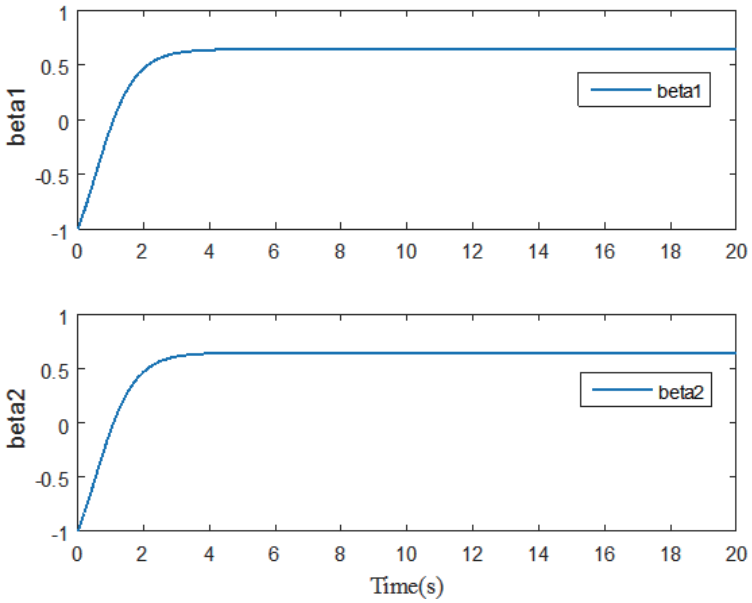

FIGURE 6. Estimate of bounds on nonlinear function β_1 and β_2

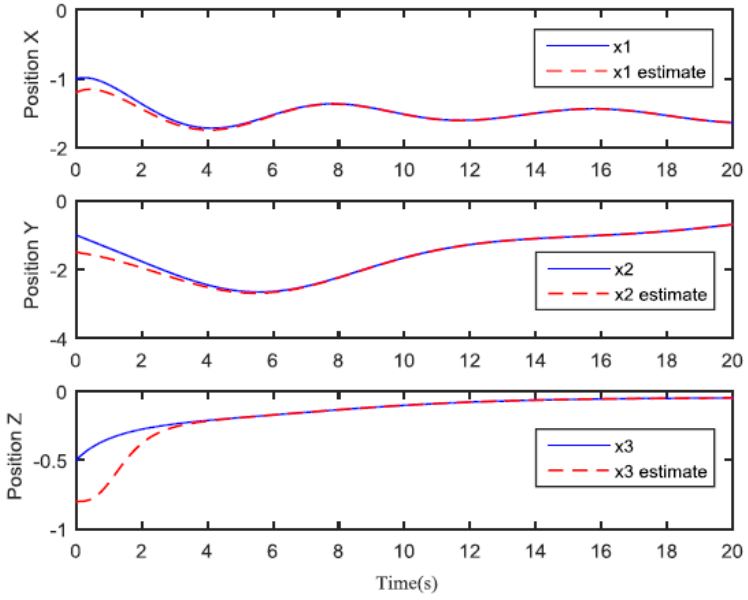

FIGURE 7. Actual and estimated positions of the dynamic object with respect to a moving camera (Case 1)

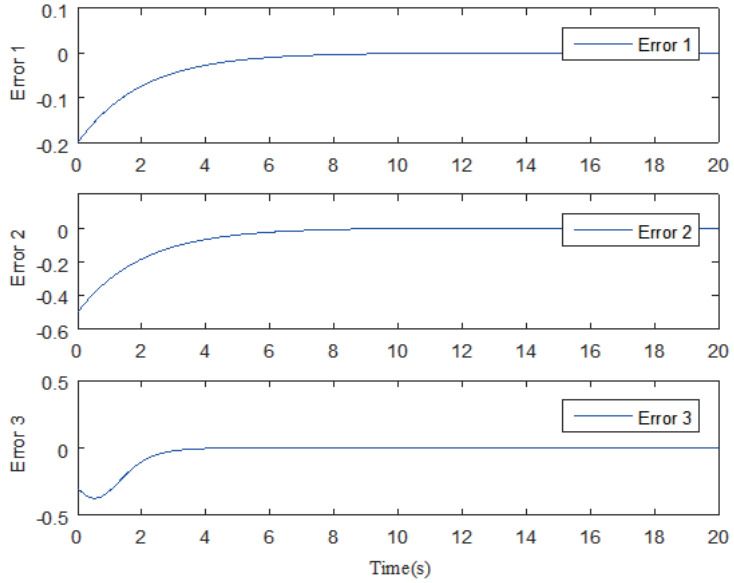

FIGURE 8. Errors in the structure estimation of the dynamic object (Case 1)

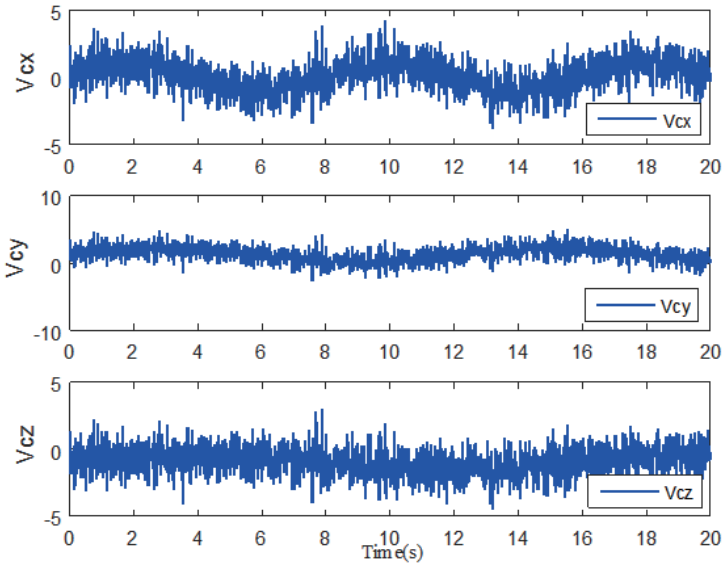

FIGURE 9. Moving camera linear velocities Vcx, Vcy and Vcz in presence of noise

Then, two cases are studied by adding noise measurements: the uncertain nonlinearities case and the uncertain nonlinearities and disturbances case.

Case 2: uncertain nonlinearities

A white noise is added to the measured camera velocities with zero mean and noise power equal to 0.01. Figure 9 shows the moving camera velocities with noises traced on the three axes of the camera frame.

Despite the presence of uncertainties, the estimated position of the moving object converges correctly to the actual ones with slight noise due to camera sensor noise, see Figure 10. The convergence time of these estimated states is slightly affected. Figure 11 delineates errors in the structure estimation. The values of errors in steady state for $\hat{x}_1$, $\hat{x}_2$

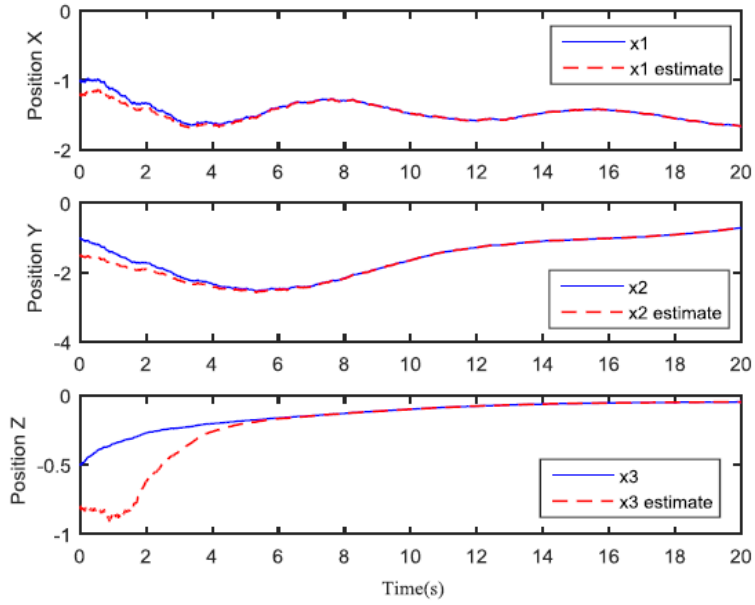

FIGURE 10. Actual and estimated positions of the dynamic object with respect to a moving camera (Case 2)

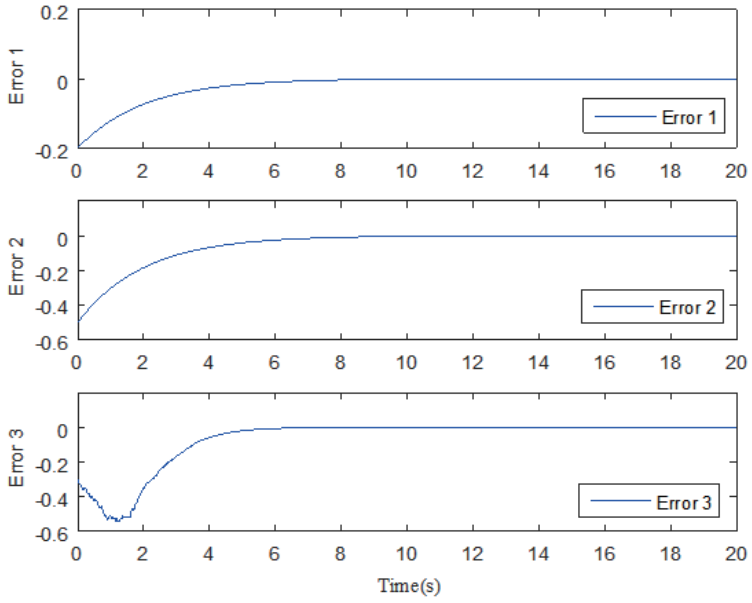

FIGURE 11. Errors in the structure estimation of the dynamic object (Case 2)

present a small difference regarding those of Case 1. The values are given as follows: $er_1 = -9.07 \times 10^{-6}$, $er_2 = -2.35 \times 10^{-5}$. For the inverse depth $\hat{x}_3$, this error has increased by 10 times compared to Case 1 but remains rather low where it is of the order of $er_3 = 0.1 \times 10^{-6}$.

Case 3: uncertain nonlinearities and disturbances

In this case, two problems are dealt with: the presence of nonlinear uncertainties and the presence of the disturbances in the unknown input due to the sensor noise.

Now, apart from the presence of uncertainties on the linear camera velocities (see Figure 9), white noise is added to the measured object velocities (see Figure 12). The last one

shows the moving object velocities with noises. Figure 13 shows comparison of the real and estimated positions of the moving object in the camera coordinate frame. However, compared with results given by the other cases, a slight noise could be observed in the components of the normalized Euclidean coordinates due to the high noise in both camera and object velocities. The errors curves in the structure estimation are exposed in Figure 14. After a convergence time, the error values remain low and they are stated as follows: $er_1 = -9.1 \times 10^{-6}$, $er_2 = -2.25 \times 10^{-5}$ and $er_3 = 8.5 \times 10^{-4}$. NUISMO was verified to function well against even the time-varying uncertainties. These results demonstrate

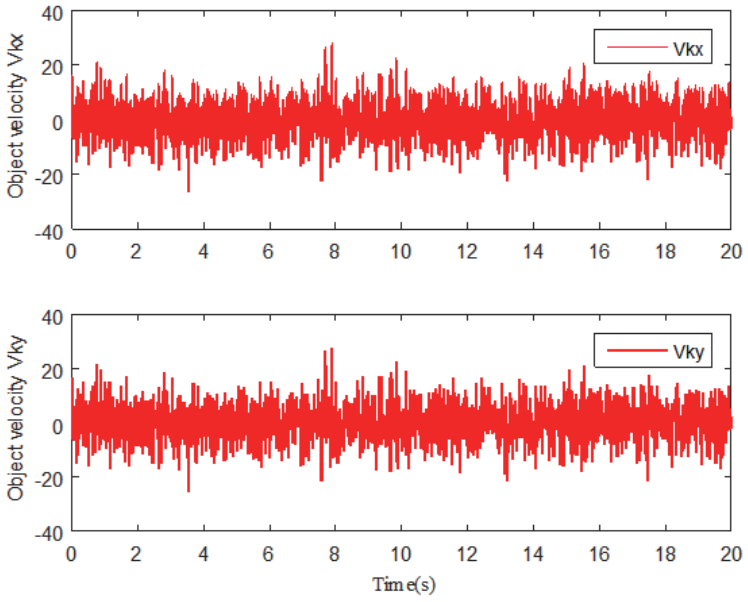

FIGURE 12. Moving object velocities Vkx and Vky in presence of noise

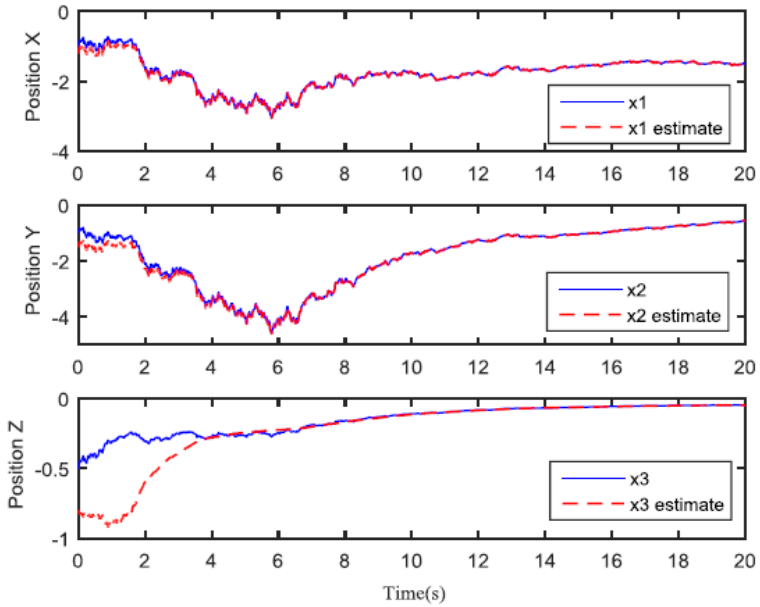

FIGURE 13. The actual and estimated positions of the dynamic object on images (Case 3)

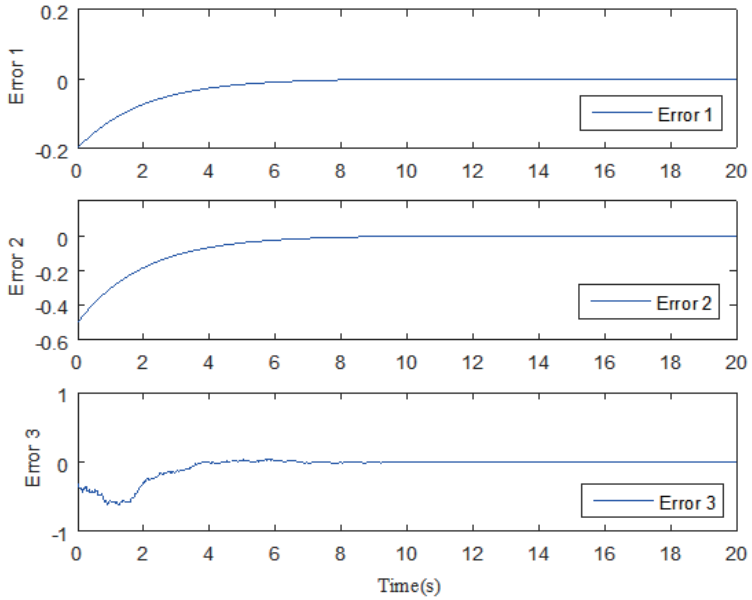

FIGURE 14. Errors in the structure estimation of a moving object (Case 3)

that the proposed approach can achieve robust and efficient performance even with the unknown object motion and measurement noise.

5. **Conclusion.** In this paper, the SaMfM problem for camera/object nonlinear system with the uncertain nonlinearities, disturbances and in the presence of unknown object velocities is investigated. The solution to this problem is defined by the proposed design NUISMO with a feedback input injection where its proven convergence is given. The dynamic system is assumed to be bounded but their bounds are unknown and are estimated adaptively using suggested laws. Unlike the previous studies, the proposed observer can be applied to the camera images of objects that move along a straight line or plane. A comparative study with an NUIO is carried out to prove the effectiveness of the proposed approach. The simulation results highlight the performances of the designed NUISMO to recover the structure of the object by presenting different simulation cases. For future works, an experimental implementation of the proposed solution can be achieved on a robot manipulator.

REFERENCES

[1] S. Avidan and A. Shashua, Trajectory triangulation: 3D reconstruction of moving points from a monocular image sequence, *IEEE Trans. Pattern Analysis and Machine Intelligence*, vol.22, no.4, pp.348-357, 2000.

[2] C. Yuan and G. Medioni, 3D reconstruction of background and object moving on ground plane viewed from a moving camera, *Proc. of IEEE Comput. Soc. Conf. Comput. Vis. Pattern Recognit.*, New York, NY, USA, pp.2261-2268, 2006.

[3] A. P. Dani, Z. Kan, N. R. Fischer and W. E. Dixon, Structure and motion estimation of a moving object using a moving camera, *American Control Conference*, Marriott Waterfront, Baltimore, MD, USA, 2010.

[4] J. A. Morgan, D. J. Brogan and P. A. Nelson, Application of Structure-from-Motion photogrammetry in laboratory flumes, *Geomorphology*, vol.276, pp.125-143, 2017.

[5] J. A. B. Lópeza, G. A. Jiménezb, M. S. Romerob, E. A. Garcíab, S. F. Martínb, A. L. Medinab and J. A. E. Guerrerob, 3D modelling in archaeology: The application of Structure from Motion methods to the study of the megalithic necropolis of Panoria (Granada, Spain), *Journal of Archaeological Science: Reports*, vol.10, pp.495-506, 2016.

[6] Z. Xu, L. Wu, M. Gerke, R. Wang and H. Yang, Skeletal camera network embedded structure-from-motion for 3D scene reconstruction from UAV images, *ISPRS Journal of Photogrammetry and Remote Sensing*, vol.121, pp.113-127, 2016.

[7] L. A. Méndez-Barroso, J. L. Zárate-Valdez and A. Robles-Morúa, Estimation of hydromorphological attributes of a small forested catchment by applying the Structure from Motion (SfM) approach, *International Journal of Applied Earth Observation and Geoinformation*, vol.69, pp.186-197, 2018.

[8] X. Wang, F. Rottensteiner and C. Heipke, Structure from motion for ordered and unordered image sets based on random k-d forests and global pose estimation, *ISPRS Journal of Photogrammetry and Remote Sensing*, vol.147, pp.19-41, 2019.

[9] J. Kaminski and M. Teicher, A general framework for trajectory triangulation, *J. Math. Imag. Vis.*, vol.21, no.1, pp.27-41, 2004.

[10] C. Yuan and G. Medioni, 3D reconstruction of background and objects moving on ground plane viewed from a moving camera, *Comput. Vision Pattern Recongnit.*, vol.2, pp.2261-2268, 2006.

[11] R. Vidal, Y. Ma, S. Soatto and S. Sastry, Two-view multibody structure from motion, *International Journal of Computer Vision*, vol.68, no.1, pp.7-25, 2006.

[12] H. Park, T. Shiratori, I. Matthews and Y. Sheikh, 3D reconstruction of a moving point from a series of 2D projections, *Euro. Conf. on Comp. Vision*, vol.6313, pp.158-171, 2010.

[13] H. Park, T. Shiratori, I. Matthews and Y. Sheikh, 3D trajectory reconstruction under perspective projection, *International Journal of Computer Vision*, vol.115, no.2, pp.115-135, 2015.

[14] F. Kahl and R. I. Hartley, Multiple view geometry under the L_∞-norm, *IEEE Trans. Pattern Analysis and Machine Intelligence*, vol.30, no.9, pp.1603-1617, 2008.

[15] R. I. Hartley and F. Kahl, Global optimization through rotation space search, *International Journal of Computer Vision*, vol.82, no.1, pp.64-79, 2009.

[16] R. Vidal and R. Hartley, Three-view multibody structure from motion, *IEEE Trans. Pattern Analysis and Machine Intelligence*, vol.30, pp.214-227, 2008.

[17] K. E. Ozden, K. Schindler and L. Van Gool, Multibody structure-from-motion in practice, *IEEE Trans. Pattern Analysis and Machine Intelligence*, vol.32, pp.1134-1141, 2010.

[18] R. Toldo, R. Gherardi, M. Farenzena and A. Fusiello, Hierarchical structure-and-motion recovery from uncalibrated images, *Computer Vision and Image Understanding*, vol.140, 2015.

[19] A. Agudo, F. Moreno-Noguer, B. Calvo and J. M. M. Montiel, Sequential non-rigid structure from motion using physical priors, *IEEE Trans. Pattern Analysis and Machine Intelligence*, vol.38, no.5, pp.979-994, 2016.

[20] A. Agudo, F. Moreno-Noguer, B. Calvo and J. M. M. Montiel, Real-time 3D reconstruction of non-rigid shapes with a single moving camera, *Computer Vision and Image Understanding*, vol.153, pp.37-54, 2016.

[21] A. P. Dani, N. Fischer and W. E. Dixon, Single camera structure and motion estimation, *IEEE Trans. Automatic Control*, vol.57, no.1, pp.241-246, 2012.

[22] A. P. Dani, Z. Kan, N. R. Fischer and W. E. Dixon, Estimating structure of a moving object using a moving camera: An unknown input observer approach, *Proc. of the IEEE Conference on Decision and Control and European Control Conference*, Orlando, FL, 2011.

[23] S. Jang, A. P. Dani, C. D. Crane and W. E. Dixon, Experimental results for moving object structure estimation using unknown input observer approach, *Annual Dynamic Systems and Control Conf. Joint with Motion and Vibration Conf.*, FL, USA, 2012.

[24] D. Chwa, A. P. Dani and W. E. Dixon, Range and motion estimation of a monocular camera using static and moving objects, *IEEE Trans. Control Systems Technology*, vol.24, no.4, pp.1174-1183, 2016.

[25] J. Keshavan and J. S. Humbert, Robust structure and motion recovery for monocular vision systems with noisy measurements, *International Journal of Control*, vol.91, no.3, pp.715-724, 2018.

[26] A. Castillo, R. Sanz, P. Garcia and P. Albertos, Robust design of the uncertainty and disturbance estimator, *IFAC-PapersOnLine*, vol.50, no.1, pp.8262-8267, 2017.

[27] A. Castillo, P. García, R. Sanz and P. Albertos, Enhanced extended state observer-based control for systems with mismatched uncertainties and disturbances, *ISA Transactions*, vol.73, pp.1-10, 2018.

[28] Q. Guo, Y. Zhang, B. Celler and S. Su, Backstepping control of electrohydraulic systems based on extended-state-observer with plant dynamics largely unknown, *IEEE Trans. Ind. Electron.*, vol.63, no.11, pp.6909-6921, 2016.

[29] H. Bay, T. Tuytelaars and L. Van Gool, SURF: Speeded up robust features, *Proc. of the 9th Eur. Conf. Comput. Vis.*, vol.3951, pp.404-417, 2006.

[30] D. G. Lowe, Distinctive image features from scale-invariant key points, *International Journal of Computer Vision*, vol.60, no.2, pp.91-110, 2004.
[31] Y. Ma, S. Soatto, J. Kosecka and S. Sastry, *An Invitation to 3-D Vision*, Springer, 2004.
[32] J. Zabczyk, Controllability and observability of nonlinear systems, *Mathematical Control Theory*, Modern Birkhäuser Classics, Birkhäuser, Boston, 2008.
[33] M. Darouach, M. Zasadzinski and S. Xu, Full-order observers for linear systems with unknown inputs, *IEEE Trans. Automatic Control*, vol.39, pp.606-609, 1994.
[34] J. Liu, S. Laghrouche and M. Wack, Finite time observer design for a class of nonlinear systems with unknown inputs, *American Control Conference*, pp.286-291, 2013.
[35] H. K. Khalil, *Nonlinear Systems*, 3rd Edition, Prentice Hall, 2002.
[36] J. G. Van Antwerp and R. D. Braatz, A tutorial on linear and bilinear matrix inequalities, *Journal of Process Control*, vol.10, no.4, pp.363-385, 2000.
[37] M. Hou, G. Duan and M. Guo, New versions of Barbalat's lemma with applications, *Journal of Control Theory and Applications*, vol.8, no.4, p.545, 2010.